THE PHYSICS OF DIFFRACTION AT HERA

B. Laforge [a]
DAPNIA/SPP, CEA/Saclay
91191 Gif sur Yvette, France
E-mail : laforge@hep.saclay.cea.fr

Recent results are described on diffractive physics from both H1 and ZEUS collaborations based on data taken both in '94 and '95. After a brief introduction to kinematics of diffraction and to the experimental apparatus at HERA, inclusive measurements such as the one of the diffractive structure function $F_2^{D(3)}$ or of the diffractive photoproduction cross section are presented. Further measurements of different exclusive final states are also discussed. Finally, we review recent results on vector meson production that show with increasing precision the transition from soft to hard production mechanisms. The structure of the pomeron ($\mathbb{P}$) can be investigated using these new available data and reveals the gluonic nature of the pomeron.

Talk given at the VII^{th} Blois conference on behalf of the H1 and ZEUS collaborations

1 Introduction

HERA is a unique facility that provides collisions between electrons (positrons) of 27.5 GeV against protons of 820 GeV, leading to a center of mass energy of about 300 GeV. In about 10% of the collisions, the incoming proton is scattered and remains intact or dissociates with a very low invariant mass so that it escapes in the beam pipe. The absence of hadronic activity between the outgoing proton and the rest of the hadronic final state is a very remarkable feature that implies the absence of color flow between these two systems. These events are interpreted as being mostly due to the exchange of a colorless object, the ($\mathbb{P}$), coupling to the proton. The data used in the presented analyzes were taken in 1994 and 1995.

1.1 The kinematics of diffraction at HERA

Diffractive exchange corresponds to the process $ep \to eXY$ where X and Y are separated by a large rapidity gap as represented on figure (1). The hadronic final state is divided into two systems X and Y, of mass M_X and M_Y, such that a color singlet exchange coupling to the $\gamma - X$ and $P - Y$ vertices can be defined. Most of the results presented here are concerned with the case where the system Y is dominantly a proton. When the system X is a bound state vector meson, the process is considered elastic at the photon vertex. Dissociation processes correspond to the cases where one or both the invariant masses M_X or M_Y of the two systems is large. The processes studied cannot directly be considered to be diffractive in the sense of the exchange of the leading vacuum singularity. Consequently, it is very important to understand the role played by non-diffractive processes in the hadron level cross-sections measured. At fixed beam energies, the kinematics of the diffractive inclusive process requires 6 independent variables. One of those is the azimuthal angle between the (e,γ) and (P,$\mathbb{P}$) planes whose distribution is assumed to be flat. Another one is M_Y which

[a] Maintenant au LPNHE-Université Paris VI, Tour 33, RdC, 4, place Jussieu, 75252 Paris cedex 5

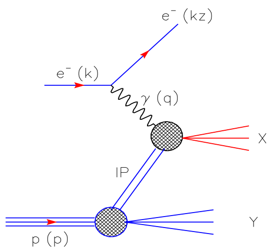

Figure 1: Kinematics of the diffractive reaction $ep \to eXY$

is supposed to be small for single dissociated events. It remains so 4 invariant variables. Those are chosen among the conventional kinematic variables x, Q^2, y and W, used to discuss inclusive ep interactions, as well as among specific variables describing the hadronic final state :

$$t = (P - Y)^2 \qquad x_{\mathbb{P}} = \frac{q.(P-Y)}{q.P} \qquad \beta = \frac{Q^2}{2q.(P-Y)} \qquad M_X^2 \tag{1}$$

where q, P, and Y are respectively the four-vectors of the incoming photon, incoming proton and outgoing system Y in the framework of figure (1). The variable t is the squared four-momentum transferred at the proton vertex, $x_{\mathbb{P}}$ is the fraction of the beam momentum transferred to the longitudinal momentum of the color singlet exchange and $\beta = x/x_{\mathbb{P}}$ (used only in the DIS regime) is the fraction of the color singlet exchange 4-momentum that is carried by the quark coupling to the photon. Depending on the different method to select the diffractive signals, the variables t and M_Y are not always measured. In any case, M_Y is restricted to be small and t is less than 1 GeV^2.

2 Experimental Equipment

The two detectors H1 and ZEUS are described in details elsewhere [1,2]. We remind only here the main characteristics of the two detectors, insisting on important features of the apparatus that are used to select diffractive events. The figures (2) and (3) show typical diffractive events in the main detector of H1 and ZEUS. These events show a clear signal in the central detectors and no hadronic activity in the forward direction (proton direction). The system X is detected in the main detector while the system Y escapes in the beam pipe and is not detected. Leading proton spectrometers (LPS) are installed both in the H1 and ZEUS experiments upstream of the interaction region as close as possible to the proton beam. These detectors are designed to be able to tag the final proton scattered in single dissociation. In addition, Forward Neutron Calorimeters were also installed to tag charged colorless exchange resulting in a neutral system Y (essentially a neutron). Addition of all these new detectors allows now a better experimental investigation of the structure of diffraction at HERA.

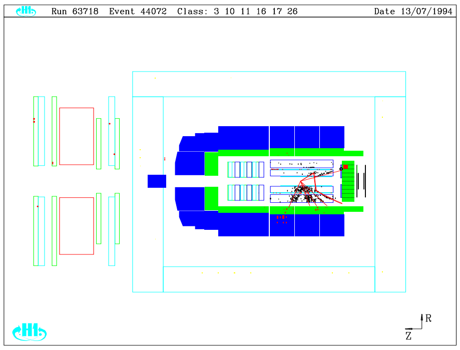

Figure 2: Event display of a typical diffractive event in the H1 detector

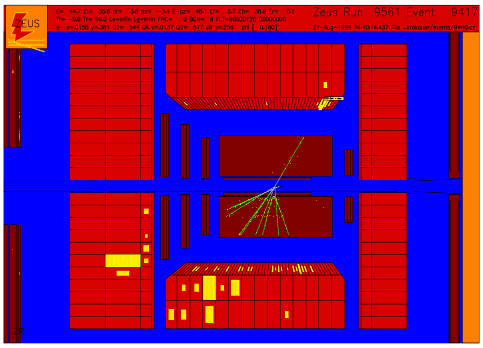

Figure 3: Event display of a high Q^2 diffractive event in the ZEUS detector

2.1 *Diffractive signals in the H1 and ZEUS detectors*

Three different methods of selecting diffractive data are now used and will be described below. The first two allow high statistics but do not have access to t and M_Y. The last one provide a full reconstruction of the kinematics but is limited in statistics by the acceptance of the LPS. These methods are :

- The rapidity gap selection method uses the central detectors as well as the forward detectors to sign the presence of a gap of rapidity between the system X seen in the central region and the system Y which escapes in the beam pipe. H1 uses its forward detectors to tag hadronic activity in the region $-1 < \eta < 7.5$. The requirement is then that the maximum pseudo-rapidity η_{max} of detected particles is less than a certain value (H1 : 3.2, ZEUS : 1.5(DIS), 4.3(γp)).

- The M_X method assumes that diffraction is linked to non exponentially suppressed processes. The selection is done by doing in each bin of interest a fit of the the M_X distribution as shown on the figure (4.a). The diffractive signal is taken as the remaining events when the exponential background is subtracted.

- The tagged proton selection makes use of LPS detectors to detect the scattered proton and to measure its energy. Figure (4.b) shows the spectrum of the longitudinal momentum fraction x_l of the beam protons carried by the outgoing protons measured by ZEUS with the LPS detector. The diffractive peak is visible around $x_l = 1$. The experimental ZEUS diffractive peak cuts correspond to the range $x_l \in [0.97, 1.02]$. x_l is related to $x_{\mathbb{P}}$ through the relation $x_l = 1 - x_{\mathbb{P}}$. The measurement of the momentum of the scattered proton allows t reconstruction with $-t \sim \frac{p_\perp^2}{x_l}$.

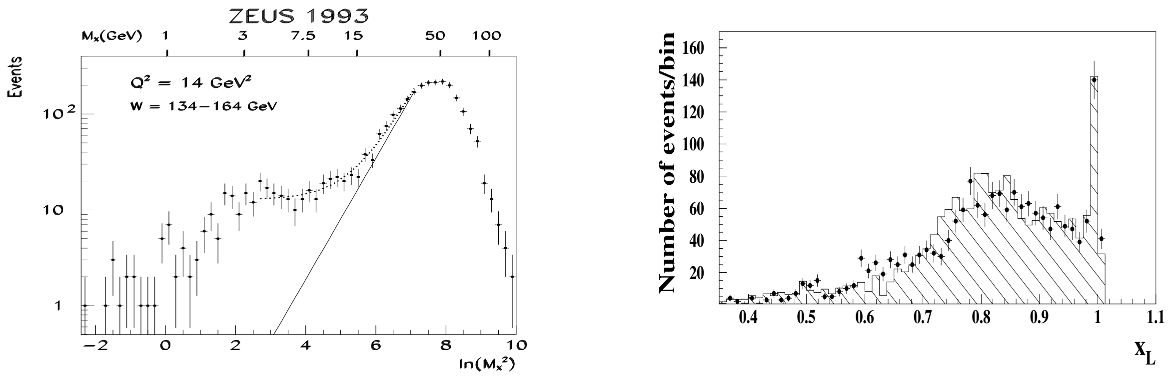

(a) (b)

Figure 4: (a) Exponential fit of the M_X distribution by ZEUS, (b) Distribution of the beam energy fraction x_l carried by the outgoing proton detected in the ZEUS LPS compared with the Monte Carlo RAPGAP based on a factorizable pomeron exchange which is able to describe the data.

3 Inclusive measurements

3.1 Diffractive Photoproduction cross-section

Figure (5.a) shows the diffractive cross-section $M_X^2 d\sigma/dM_X^2$ versus M_X^2 in the photoproduction regime measured by H1 in two bins of W^2. Figure (5.b) presents the ZEUS cross-section $1/\sigma_{tot} d\sigma/d\ln M_X$ as a function of M_X at $W \sim 200$ GeV. The H1 results are integrated over $|t| < 1$ GeV and $M_Y < 1.6$ GeV, the ZEUS results over $M_Y < 2.$ GeV and all $|t|$. A triple Regge approach is taken by both collaborations, such that the M_X and W dependences of the cross-section can be parameterized as[3,5] :

$$\frac{d\sigma}{dtdM_X^2} = \frac{s_o}{W^4} \sum_{i,j,k} G_{ijk}(t) \left(\frac{W^2}{M_X^2}\right)^{\alpha_i(t)+\alpha_j(t)} \left(\frac{M_X^2}{s_o}\right)^{\alpha_k(0)} cos[\Phi_i(t) - \Phi_j(t)] \qquad (2)$$

where i and j correspond to the physical reggeon coupling to the proton ($i \neq j$ for interference terms) and k is a further reggeon describing the forward elastic amplitude $\gamma\alpha_i \to \gamma\alpha_j$ at a centre of mass energy given M_X. The hadronic scale s_o is taken to be 1 GeV^2, $\Phi_i(t)$ is the phase of reggeon i, specified by its signature factor, and $G_{ijk}(t)$ contains all the couplings in the triple Regge amplitude involving reggeons i, j and k. The main contribution comes from the triple $\mathbb{P}$ vertex, but even at large W^2, the Reggeon contribution is found to be not negligible. The interference terms involving two reggeon and one pomeron (or the reverse) are found to have a noticeable contribution increasing with M_X^2. ZEUS fit only a triple pomeron term[6] for different M_X ranges. The result is shown on top of the ZEUS cross-section and seems to be unstable showing that this distribution cannot be fitted with only a triple $\mathbb{P}$ exchange. There is a need for a reggeon term to have a stable result. Both H1 and ZEUS obtain then the result that the pomeron intercept extracted from these data is compatible

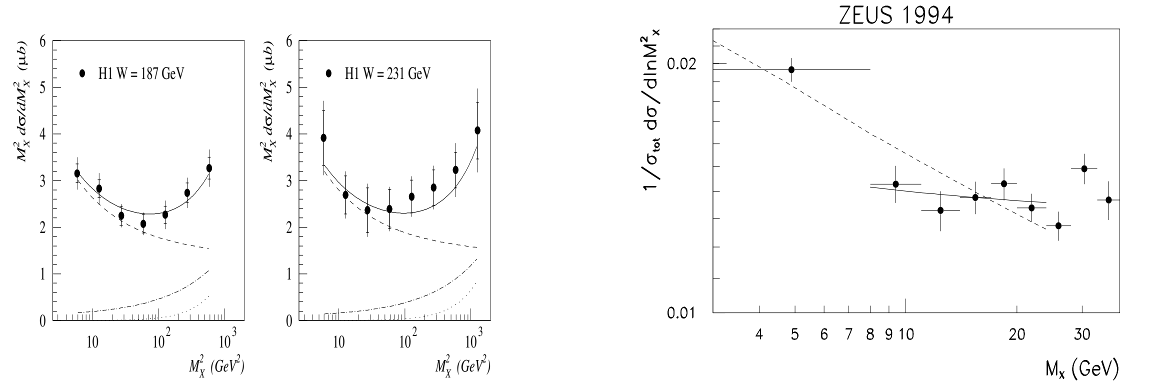

(a) (b)

Figure 5: H1 and ZEUS measurement of the M_X dependence of the diffractive photoproduction cross-section. (a) Triple vertex H1 analysis : all terms (full), diffractive terms (dashed), interference terms (dashed-dotted), non diffractive terms (dotted), (b) ZEUS pomeron triple vertex fit in different M_X ranges : $M_X \in [3, 24]$ GeV (dashed),$M_X \in [8, 24]$ GeV (full)

to the one describing hadron-hadron and photoproduction elastic and total cross-sections at high energy. H1 obtain $\alpha_{\mathbb{P}} = 1.068 \pm 0.016(stat.) \pm 0.022(syst.) \pm 0.041(model)$ where the model dependence error is dominated by uncertainties on the sub-leading terms. The ZEUS result is $\alpha_{\mathbb{P}} = 1.12 \pm 0.04(stat.) \pm 0.08(syst.)$.

ZEUS used also its LPS to measure the t dependence of diffractive photoproduction for $0.07 < |t| < 0.4$ GeV^2, $4 < M_X < 32$ GeV and $< W > \sim 200$ GeV. The result is $b = 7.3 \pm 0.9 \pm 1.0$ GeV^{-2}, a little larger than the one measured at $< W > \sim 14$ GeV [4] and consistent with shrinkage of the forward diffractive peak with $\alpha'_{\mathbb{P}} = 0.25$ GeV^{-2}.

3.2 Diffractive Deep Inelastic Scattering cross-section

H1 measurement of $F_2^{D(3)}$

The cross-section of the semi-inclusive process $ep \to eXY$ can be written using the analogy to the proton structure F_2 by :

$$\frac{d^3\sigma_{ep\to eXY}}{dx_{\mathbb{P}}\,d\beta\,dQ^2} = \frac{4\pi\alpha^2}{\beta Q^4}\left(1 - y + \frac{y^2}{2}\right)F_2^{D(3)}(\beta, Q^2, x_{\mathbb{P}}) \tag{3}$$

A Regge approach is taken to parameterize the $x_{\mathbb{P}}$ dependence such that $F_2^{D(3)}$ decomposes into contributions of different trajectories $\alpha_i(t) = \alpha_i(0) + \alpha'_i t$ according to :

$$F_2^{D(3)}(\beta, Q^2, x_{\mathbb{P}}) = \sum_i \int_{-1\ \mathrm{GeV}^2}^{t_{min}} dt\ e^{b_o^i t}\left(\frac{1}{x_{\mathbb{P}}}\right)^{2\alpha_i(t)-1} A^i(\beta, Q^2) \tag{4}$$

where $A^i(\beta, Q^2)$ is proportional to the structure function of the exchange i and b_o^i is the logarithmic slope of the t dependence of the coupling of the exchange i to the photon and the proton. For each of the separate exchanges, the $x_{\mathbb{P}}$ dependence then factorizes from the β and Q^2 dependence.

With '94 data[7], H1 measured $F_2^{D(3)}$ over the range $2.5 < Q^2 < 65$ GeV^2, $0.01 < \beta < 0.9$, $0.0001 < x_{\mathbb{P}} < 0.05$, $M_p < M_Y < 1.6$ GeV, and $t_{min}(\sim 10^{-3}) < |t| < 1$GeV^2. Figure (6.a) shows $x_{\mathbb{P}} F_2^{D(3)}$ in two particular bins in β for $Q^2 = 20$ GeV^2. A single Regge approach is used to analyze the experimental data with two contributions since a single $\mathbb{P}$ exchange leads to a factorization breaking where the effective $\alpha_{\mathbb{P}}$ increases with β (H1 sees no dependence with Q^2). The analysis includes also an interference term with a phase of 45 degrees, such that a fit of $F_2^{D(3)}$ is done with the following functional form :

$$F_2^{D(3)} = F_2^{\mathbb{P}}.x_{\mathbb{P}}^{-n1} + C_M.F_2^M(\beta, Q^2).x_{\mathbb{P}}^{-n2} + \text{interference term} \qquad (5)$$

The result of the fit gives $n_1 = 1.29 \pm 0.03 \pm 0.06 \pm 0.03$(model) and $n_2 = 0.3 \pm 0.3 \pm 0.6 \pm 0.2$(model), the meson intensity C_M and $F_2^{\mathbb{P}}(\beta, Q^2)$. $F_2^{\pi}(GRV)$ was used for the meson structure function. Since $n = 2\alpha_i - 1$, these results correspond then to $\alpha_{\mathbb{P}} = 1.18 \pm 0.02 \pm 0.04$ and $\alpha_M = 0.6 \pm 0.1 \pm 0.3$. The second trajectory intercept is consistent with the approximately degenerate ρ, ω, f and a trajectory that are necessary to describe total cross-sections. A second step is done doing a QCD analysis of the extracted $\mathbb{P}$ structure function. This analysis based on DGLAP evolution is analogous to the usual QCD analysis of the proton structure F_2. The parton densities resulting from this QCD fit are shown at $Q^2 = 5$ GeV^2 on figure (6.b). The $\mathbb{P}$ appears to be a gluonic object with a gluon density peaked at high values of $x_{i/\mathbb{P}}$, the momentum fraction of the pomeron carried by the gluon involved in the hard process. The dominating picture is then a pomeron behaving as a leading gluon hidden in a cloud of partons neutralizing the color field. The gluons are found to carry about 80 % of the $\mathbb{P}$ momentum over the all range in Q^2.

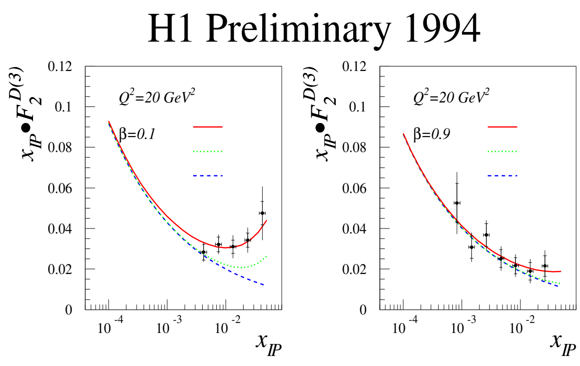

(a)

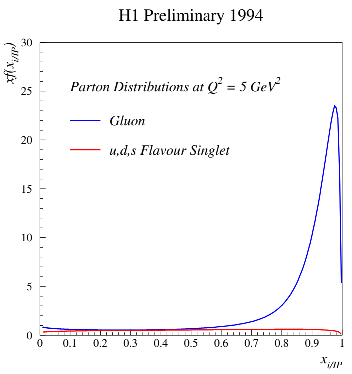

(b)

Figure 6: (a) H1 diffractive structure function measurement for two bins in β and Q^2. On top of the data is overlaid the result of a Regge based phenomenological fit. Upper line : all contributions, Intermediate line : $\mathbb{P}$ + meson , lower line : $\mathbb{P}$ only. (b) Gluon (peak) and quark densities in the $\mathbb{P}$ from the QCD fit of $F_2^{D(3)}$.

ZEUS measurement of $\frac{d\sigma}{dM_X}$ versus W

Using the M_X selection method, ZEUS measurement[8] of the diffractive $\gamma p \rightarrow XY$ cross-section in different bins in M_X as a function of W is presented on the figure (7.a) and shows a steep dependence of this cross section with W. This measurement is achieved over the range $8 < Q^2 < 60$ GeV^2, $0.028 < \beta < 0.94$, $0.7 \lesssim M_X < 15$ GeV, $M_p \leq M_Y < 4$ GeV, and all $|t|$ with $< |t| >\sim 0.18$ GeV^2. A Regge inspired fit to this cross section has been done using a power law in W^2 of the form $(W^2)^{2(\alpha_{\mathbb{P}}-1)}$. Figure (7.b) presents the dependence of the fitted effective $\alpha_{\mathbb{P}}$ with Q^2 in two bins of M_X. There is a tendency of this exponent to grow with Q^2 but more data are needed to draw a clear conclusion. At the present stage, these results are in agreement within the errors with the $H1$ measurement of $\alpha_{\mathbb{P}}$.

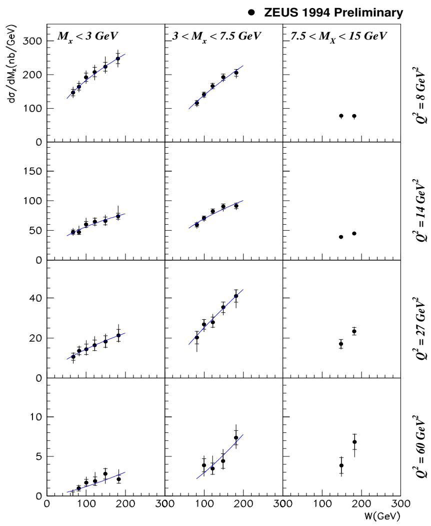

(a)

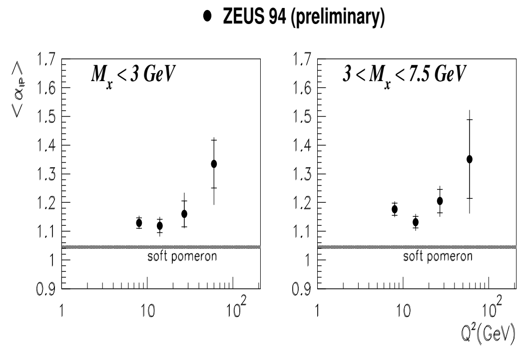

(b)

Figure 7: (a) Diffractive $\frac{d\sigma_{\gamma p \rightarrow XY}}{dM_X}$ as a function of W in different bins in Q^2 and M_X as measured by ZEUS. A fit with a power law is put on top of the data, (b) evolution of the power law exponent with Q^2.

ZEUS measurement of events with a tagged proton

The ZEUS collaboration also used the LPS detector to measure the diffractive structure function [9] over the domain $4.10^{-4} < x_{\mathbb{P}} < 3.10^{-2}$, $4 < Q^2 < 20$ GeV^2, $0.006 < \beta < 0.5$ and $0.07 < |t| < 0.35$ GeV^2. The main advantages of this method are that it tags exactly events with a proton in the final state and that it increases the acceptance in M_X and improves the reconstruction of the kinematics. Unfortunately, the statistics are very low due to the low acceptance of the LPS. Consequently, the present measurement of $x_{\mathbb{P}} F_2^{D(3)}$ is integrated over t. This measurement is presented on the figure (8). A fit with power law in $x_{\mathbb{P}}$ leads

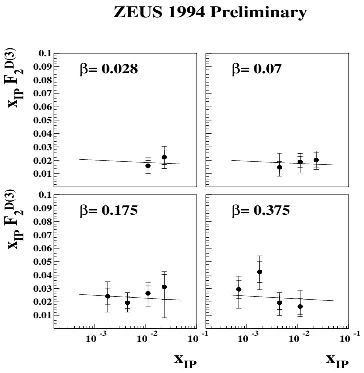

Figure 8: Diffractive structure function from the ZEUS LPS data as a function of $x_{\mathbb{P}}$ for different bins in β. A power law fit is shown on top of the measurement with an exponent $n = 1.04 \pm 0.09 \pm 0.14$.

to an exponent $n = 1.04 \pm 0.09 \pm 0.14$. Note the different kinematic region covered by that measurement sitting at rather high $x_{\mathbb{P}}$ where the reggeon contribution can be important and favors a smaller value of n than for the rapidity gap selection range. On the other hand, ZEUS could also measure the t dependence [10] of the diffractive electroproduction cross-section and obtains $b = 7.11 \pm 1.1^{+0.7}_{-1.1}$.

4 Exclusive measurements

Exclusive measurements are another way to test the mechanism of diffraction and to prove our understanding of the structure of the $\mathbb{P}$. Some of these processes give an occasion to apply perturbative QCD and to compare it to the data. The diffractive exclusive processes which have been measured at HERA are di-jet production and elastic vector meson production both in the photoproduction or electroproduction regime. Di-jet production is predominantly sensitive to the gluon density inside the pomeron through the boson-gluon fusion hard subprocess although it is also sensitive to the quark density through the QCD-Compton subprocess.

4.1 Diffractive di-jets production

Figure (9.a) presents the ZEUS measurement of the diffractive di-jet photoproduction cross section [11] versus the pseudo-rapidity of the jets. This measurement is compared with various hypotheses on the structure of the $\mathbb{P}$. Data favors a hard or super-hard gluon structure of the pomeron. Different other differential di-jet cross sections have been measured by ZEUS and are used together with the '93 ZEUS measurement [12] of $\tilde{F}_2^D$ (the integration of $F_2^{D(3)}$ over the measurement $x_{\mathbb{P}}$ range) to have further information on the parton densities inside the $\mathbb{P}$. The best fits are presented figure (9.b) on top of the data which favors a hard gluon structure of the $\mathbb{P}$ and points out that more than 70 % of the pomeron momentum is carried

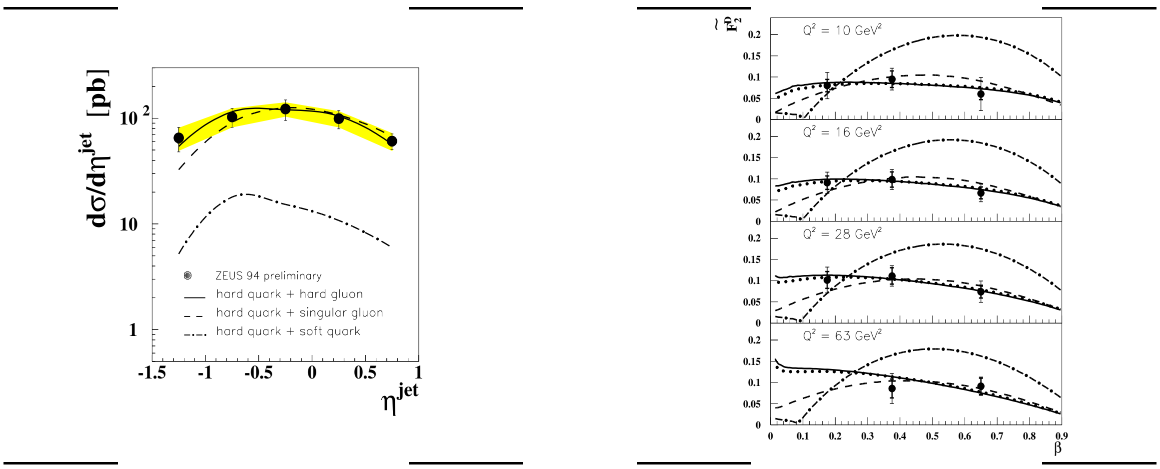

(a) (b)

Figure 9: (a) ZEUS di-jet cross section in diffractive photoproduction versus the pseudo-rapidity of the jet in the lab frame, (b) ZEUS measurement of $\tilde{F}_2^D(\beta, Q^2)$ as a function of β for different Q^2. Best fit result with different assumptions of the $\mathbb{P}$ parton densities are overlaid.

by the gluons. These observations are in agreement with the conclusions of the H1 QCD analysis of $F_2^{D(3)}$[13]. Figure (10) shows the H1 diffractive di-jet $(ep \to X(jet-jet)Y)$ cross section measurement[14] done both in the photoproduction and electroproduction regime as a function of $\xi_{\mathbb{P}}$, the momentum fraction of the $\mathbb{P}$ carried by the di-jet system measured at the hadron level. At the parton level, $\xi_{\mathbb{P}}$ would be the momentum fraction of the $\mathbb{P}$ carried

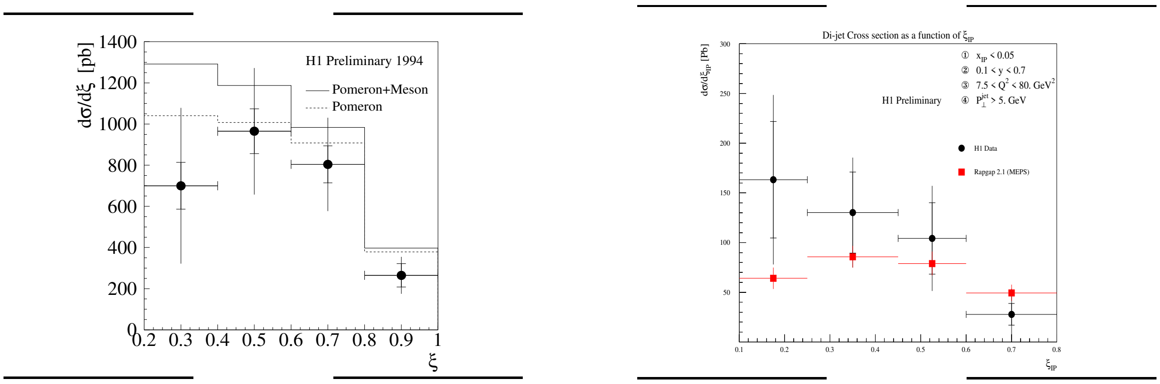

(a) (b)

Figure 10: (a) H1 di-jet cross sections in diffractive photoproduction (a) and in diffractive DIS (b) versus $\xi_{\mathbb{P}}$. The overlaid predictions are obtained using the $\mathbb{P}$ parton densities taken from QCD analysis of $F_2^{D(3)}$.

by the parton going into the hard subprocess. No significant exclusive di-jet contribution is seen at high $\xi_{\mathbb{P}}$. Consequently, there is no evidence of any result which could be related to the super-hard contribution of the kind reported by UA8 [15] nor any evidence for 2-gluon exchange processes leading to exclusive di-jet production[16]. Predictions made with

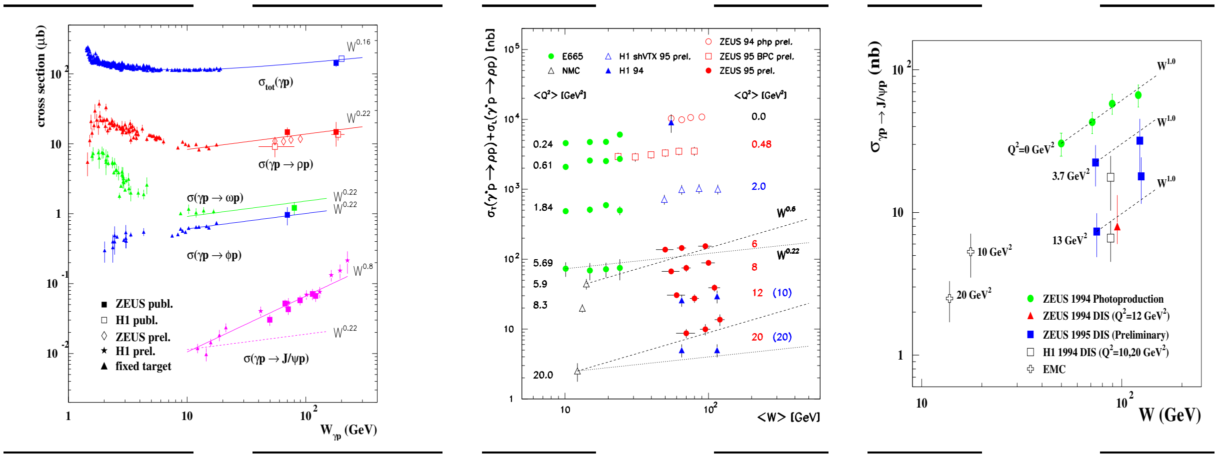

(a) (b) (c)

Figure 11: Vector Meson cross sections in photoproduction (a) and in DIS (b,c)

the help of H1 QCD-fit $\mathbb{P}$ parton densities through the RAPGAP (DIS) and POMPYT (photoproduction) Monte Carlos describe fairly well the data. In photoproduction, clear contributions from resolved and direct photon processes are observed.

4.2 Vector meson production

Many results[17] on vector meson production have been obtained by H1 and ZEUS and I do have not the place to cover them all. In this report, I will concentrate on the energy dependence of such processes. The figure (11.a) summarizes the W dependence of different meson vector photoproduction cross sections. For all vector mesons except the J/Ψ, the W dependence can be reproduced by a soft pomeron behavior just as the total γp cross section. The steeper J/Ψ W dependence can be described by QCD predictions where the perturbative scale is related to the squared mass of the charm quark. The figure (11.b) and (11.c) show respectively the W dependence of the ρ and the J/Ψ for different bins in Q^2. For the ρ, the situation is unclear at the moment due to discrepancies different data sets. For the J/Ψ, the W dependence is similar to its photoproduction behavior. A change on the W dependence with Q^2 would be the sign of a transition from a non perturbative process described by the vector dominance model at $Q^2 = 0$ to a perturbative one where the scale is given by Q^2.

5 Conclusions

A significant amount of data on diffractive processes has been measured by the H1 and ZEUS experiments whose analysis give a better understanding of the nature of the $\mathbb{P}$. There is now agreement that the value of the intercept of the $\mathbb{P}$ is significantly higher in the high Q^2 regime than the one extracted in photoproduction or from soft hadron-hadron physics. There is also a consensus from two independent analyzes from H1 and ZEUS that the $\mathbb{P}$ is a gluon dominated object whose gluons carries more than 70% of its momentum and which can be see as a leading gluon at low scale. The new vector meson production data increase the precision with which the transition from the vector dominance to the perturbative region is measured.

Acknowledgments

I want to thank here both experiment H1 and ZEUS for their trust. I also thank the HERA machine people, engineers without who none of these results would be there. I thank J. Dainton, J. Phillips, A. Mehta, P. Newman, P. Marage, R. Nania and E. Gallo for fruitful discussions during the preparation of this talk.

References

1. The H1 Detector at HERA (Updated Version), H1 Collaboration, I. Abt *et al.*, *Nucl. Instrum. Methods* A **386**, 310 (1997).
2. ZEUS: A Detector for HERA, D. Notz (DESY). 1990, In Kazimierz 1990, Proceedings, Physics of elementary interactions, 500-510.
3. H1 Collaboration, C. Adloff *et al*, *Z. Phys.* C **74**, 221 (1997)
4. T. Chapin *et al.*, *Phys. Rev.* D **31**, 17 (1985)
5. A. Kaidalov, *Phys. Rep.* **50**, 157 (1979),
   G. Alberi, G. Goggi, *Phys. Rep.* **74**, 1 (1981),
   K. Goulianos, *Phys. Rep.* **101**, 169 (1983),
   N. Zotov, V. Tsarev, *Sov. Phys. Usp.* **31**, 119 (1988).
6. ZEUS Collaboration, J. Breitweg *et al*, DESY **97-061**, to appear in *Z. Phys.*.
7. H1 Collaboration, contribution pa02-61 to the 28th International Conference on High Energy Physics, July 1996, Warsaw, Poland.
8. G. Briskin, Proceedings of the conference DIS '97, Chicago, 1997.
9. Emanuela Barberis, contribution to the conference DIS 96, Rome, 1996.
10. ZEUS Collaboration, contribution pa02-026 to the 28th International Conference on High Energy Physics, July 1996, Warsaw, Poland.
11. J. Terron, Proceedings of the conference DIS '97, Chicago, 1997.
12. ZEUS Collaboration, M. Derrick *et al.*, *Z. Phys.* C **68**, 569 (1995)
13. J. Phillips, Proceedings of the conference ICHEP '96, Warsaw, 1996.
14. P. Marage, Proceedings of the conference DIS '97, Chicago, 1997.
15. UA8 Collaboration, R. Bonino *et al.*, *Phys. Lett.* B **211**, 239 (1988),
    UA8 Collaboration, A. Brandt *et al.*, *Phys. Lett.* B **297**, 417 (1992).
16. J. Bartels, H. Lotter et M. Wüsthoff, DESY 96-026, hep-ph/9602363, (1996),
    J. Bartels, C. Ewers, H. Lotter et M. Wüsthoff, DESY 96-085, hep-ph/9605356, (1996).
17. L. Adamczyk, Proceedings of the conference DIS '97, Chicago, 1997,
    T. Monteiro, Proceedings of the conference DIS '97, Chicago, 1997,
    F. Gaede, Proceedings of the conference DIS '97, Chicago, 1997,
    ZEUS Collaboration, M. Derrick *et al.*, *Phys. Lett.* B **377**, 259 (1996),
    ZEUS Collaboration, M. Derrick *et al.*, *Z. Phys.* C **73**, 73 (1996).